Chemical Science

ROYAL SOCIETY OF CHEMISTRY

EDGE ARTICLE

View Article Online
View Journal | View Issue

Check for updates

Cite this: *Chem. Sci.*, 2020, **11**, 2121

All publication charges for this article have been paid for by the Royal Society of Chemistry

Received 2nd December 2019
Accepted 13th January 2020

DOI: 10.1039/c9sc06089h

rsc.li/chemical-science

Enantioselective oxygenation of exocyclic methylene groups by a manganese porphyrin catalyst with a chiral recognition site†

Finn Burg, Stefan Breitenlechner, Christian Jandl and Thorsten Bach *

The natural enzyme cytochrome P450 is widely recognised for its unique ability to catalyse highly selective oxygen insertion reactions into unactivated C–H bonds under mild conditions. Its exceptional potential for organic synthesis served as an inspiration for the presented biomimetic hydroxylation approach. *Via* a remote hydrogen bonding motif a high enantioselectivity in the manganese-catalysed oxygenation of quinolone analogues (27 examples, 18–64% yield, 80–99% ee) was achieved. The site-selectivity was completely altered in favour of a less reactive but more accessible position.

Introduction

The direct functionalisation of carbon hydrogen (C–H) bonds unambiguously belongs to the most coveted transformations in modern organic synthesis.[1] The C–H bond activation of sp^3 carbon centres presents a significant challenge due to the inert nature of hydrocarbons and due to the desired distinction between the various aliphatic C–H bonds embodied in organic molecules.[2] In this context, the hydroxylation of prochiral methylene compounds poses an additional conundrum, as the corresponding secondary alcohol should ideally be formed as a single enantiomer without subjecting the newly generated stereogenic centre to an additional oxidation step.[3,4] Inspired by the remarkable efficiency of enzymatic oxygenations catalysed by cytochrome P450,[5] there are numerous examples of transition metal complexes, containing salen,[6,7] porphyrin,[8,9] and aminopyridine ligands[10,11] which have been employed in the oxygenation of C–H bonds. Since in many cases the chirality is transferred by a bulky ligand, it is perhaps not surprising that such a sterically demanding environment can be repulsive thus resulting in an insufficient conversion. Unlike its natural occurring congeners, these systems lack a favourable substrate–catalyst orientation which in turn facilitates an enantioselective approach to the substrate while maintaining a high turnover.

In recent years, it has been realised that the quest for enantio- and site-selective oxygenation reactions at remote positions (remote functionalisation) can be successfully tackled by catalysts with a non-covalent recognition element.[12] After seminal work by Breslow and co-workers on selective oxidation and oxygenation reactions,[13] notable contributions have been made among others by the groups of Groves,[14] Crabtree,[15] and Costas.[16] An early example that demonstrated how recognition elements can control selectivity in epoxidation reactions was reported by the group of Breslow (Fig. 1a).[13b] They used a manganese salen complex, that was functionalised by a chelating dipyridine moiety inviting coordination of other metals. In a competing experiment of a nicotinyl- and a benzoyl-substituted olefin, a very high selectivity (>20 : 1) was achieved

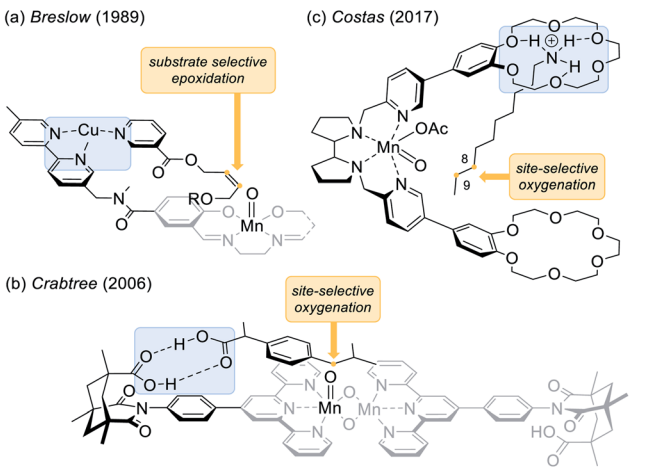

Fig. 1 Controlling selectivity in oxidation and oxygenation reactions *via* supramolecular recognition. (a) Substrate selective epoxidation of nicotinic acid derivatives controlled by complexation of copper ions. (b) Site-selective oxygenation of ibuprofen mediated by two-point hydrogen bonding between two carboxylic acids. (c) Site-selective oxygenation of ^{n}decylamine directed by a 18-crown-6 functional group.

Department Chemie, Catalysis Research Center (CRC), Technische Universität München, 85747 Garching, Germany. E-mail: thorsten.bach@ch.tum.de; Fax: +49 89 28913315; Tel: +49 89 28913330

† Electronic supplementary information (ESI) available: Synthetic procedures and full characterisation for all starting materials and products (**2**–**10**), spectroscopic data, NMR spectra, kinetic studies, *etc.* CCDC 1967795. For ESI and crystallographic data in CIF or other electronic format see DOI: 10.1039/c9sc06089h

Open Access Article. Published on 14 January 2020. Downloaded on 2/24/2026 2:58:26 PM. This article is licensed under a Creative Commons Attribution-NonCommercial 3.0 Unported Licence.

Open Access Article. Published on 14 January 2020. Downloaded on 2/24/2026 2:58:26 PM.
This article is licensed under a Creative Commons Attribution-NonCommercial 3.0 Unported Licence.

for the epoxidation of the former derivative in the presence of Cu^{2+} ions indicating that pre-coordination *via* complexation of the pyridine residues enhanced the reaction.

A contribution by Crabtree[15a] and co-workers (Fig. 1b) made intentional use of hydrogen bonds as an operative tool to control selectivity in oxygenation reactions. In this specific case, a di-μ-oxo dimanganese centre is flanked by two terpyridine ligands, which in turn are connected to a molecular recognition unit derived from Kemp's triacid.[17,18] The presented site-selective oxygenation of ibuprofen can thus be rationalised by a two-point hydrogen bonding between the two carboxylic acids. In a more recent example, the group of Costas employed a manganese aminopyridine ligand that was functionalised with two 18-crown-6 ether units (Fig. 1c).[16b] The remote crown ether effectively anchors the ^{n}decylamine at the terminal ammonium ion whereupon a selective oxygenation at carbon atoms C-8 and C-9 is induced.

Although it was beyond the intended scope of the above-mentioned catalysts to differentiate between enantiotopic hydrogen atoms, there have been several reports in which hydrogen bonding was invoked as the key element to induce enantioselectivity in catalysis.[19,20] However, examples remain scarce in which both the site- and the enantioselectivity of oxygenation reactions were successfully addressed.[21] In recent years, our group has designed and synthesised bifunctional ligands with which a catalytically active metal centre is tailored to a chiral lactam[22] recognition unit. Originally conceived for applications in photochemistry the concept of two-point hydrogen bonding[23] has successfully been applied to enantioselective olefin addition[24] and C–H functionalisation[25] reactions. As a recent supplement to this type of catalysts we prepared the chiral manganese porphyrin complex **1**[25c] for an application to enantioselective oxygenation reactions (Fig. 2, left).

In the present study we report a general bioinspired approach towards the site- and enantioselective oxygenation of a vast array of 3-benzyl and 3-alkyl substituted quinolones displaying an exocyclic methylene group (Fig. 2, right). Despite the free rotation around the quinolone–methylene bond C–H oxygenations occurred with high enantioselectivities (up to 99% ee). Some of the quinolone substrates were also probed in a racemic oxygenation reaction using manganese(III)-5,10,15,20-tetrakis(pentafluorophenyl)porphyrin chloride (Mn[TPFPP]Cl), whereupon the conversion decreased drastically, suggesting that the non-covalent hydrogen bonding interactions have also a rate accelerating effect. Most importantly, in the case of a second reactive benzylic position, the site-selectivity of the racemic reaction was reverted compared to the hydrogen bond-mediated system. This observation indicates that hydrogen bonds direct the oxygenation event to a previously inaccessible carbon centre, while the intrinsically more reactive position remains intact.

Results and discussion

Our work commenced with an investigation into the enantioselective oxygenation of the literature-known 3-(4′-methylbenzyl)quinolone (**2a**)[25a] under our previously optimised reaction conditions (Scheme 1, $t = 16$ h).[25c] We were delighted to observe that the enantiomeric excess in the exocyclic oxygenation was exceptionally high (95% ee) when employing 2.0 mol% of porphyrin **1** and iodosobenzene as a stoichiometric oxidant. The reaction delivered the desired alcohol **3a**, which was accompanied by ketone **4a**, the product of over-oxidation. It was quickly realised, though, that the catalytic activity decreased significantly before even less than half of the starting material **2a** was consumed. The alcohol to ketone ratio (**3a**/**4a** = 70/30) after 4 h was relatively low compared to the ratio we had observed in related studies and accordingly we sought for ways to improve the mass balance while concomitantly increasing the catalytic turnover.

One promising approach that caught our attention was to use an excess of the lactam **2a** relative to the oxidant. In this instance, an even lower catalyst loading of 1.0 mol% was sufficient to generate a significantly higher alcohol concentration (Fig. 3), and simultaneously the alcohol to ketone ratio improved notably (**3a**/**4a** = 80/20).

We continued with our optimisation using the oxidant iodosobenzene as the limiting reagent in a dichloromethane solution and varied the amount of quinolone **2a** applied (Table 1, entries 1 and 2). With 2.0 equivalents, the alcohol to ketone ratio deteriorated (**3a**/**4a** = 76/24) and it seemed warranted to keep the concentration of the substrate – which was readily available on gram scale – high. An increase or decrease of the substrate concentration c led to a lower enantioselectivity (entries 3 and 4), while a higher catalyst loading turned out to be

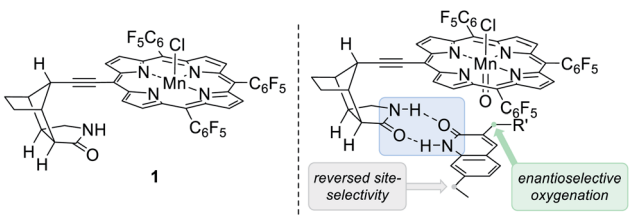

Fig. 2 Structure of the manganese porphyrin complex **1** exhibiting a chiral lactam recognition unit (left). Proposed transition state for the oxygenation of exocyclic methylene groups in quinolone analogues where hydrogen bonding effectively induces enantioface differentiation (right).

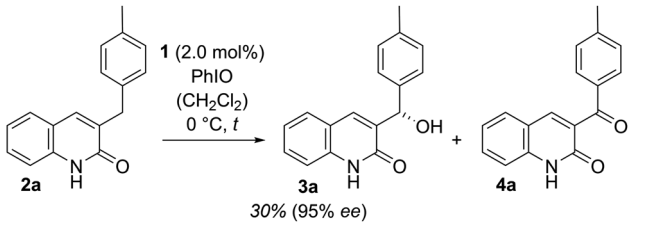

Scheme 1 Enantioselective oxygenation of 3-(4′-methylbenzyl)quinolone (**2a**) to alcohol **3a** and ketone **4a** catalysed by the chiral manganese porphyrin **1** under previously reported conditions (initial experiment, see also Fig. 3 and the narrative).[25c]

This journal is © The Royal Society of Chemistry 2020

Open Access Article. Published on 14 January 2020. Downloaded on 2/24/2026 2:58:26 PM.
This article is licensed under a Creative Commons Attribution-NonCommercial 3.0 Unported Licence.

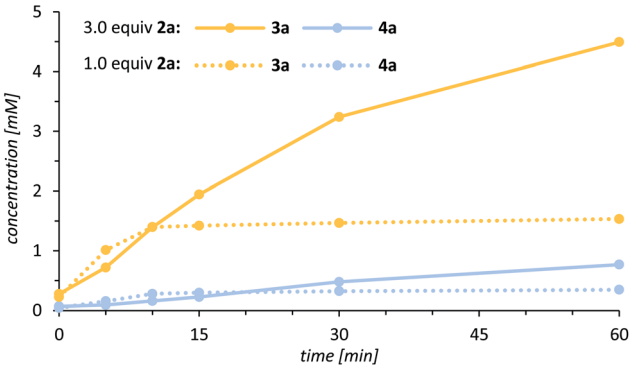

Fig. 3 Rate profile for the oxygenation of 3-(4′-methylbenzyl)quinolone (**2a**) to alcohol **3a** (yellow) and ketone **4a** (blue) catalysed by 1.0 mol% of the chiral manganese porphyrin complex **1** [0 °C, CH_2Cl_2, solid line = 3.0 equiv. of **2a**, 1.0 equiv. PhIO (c = 10 mM); dashed line = 1.0 equiv. of **2a** (c = 10 mM), 2.0 equiv. PhIO].

Table 1 Optimisation of the enantioselective oxygenation of 3-(4′-methylbenzyl)-quinolone (**2a**) catalysed by the chiral manganese porphyrin complex **1** (DCE = 1,2-dichloroethane)

Entry[a]	c[b] [mM]	**1** [mol%]	Solvent	**3a**[c] [%]	% ee[d]	**4a**[c] [%]
1	30	1.0	CH_2Cl_2	48	91	11
2[e]	20	1.0	CH_2Cl_2	42	93	13
3	20	1.0	CH_2Cl_2	39	86	11
4	60	1.0	CH_2Cl_2	50	87	12
5	30	2.0	CH_2Cl_2	48	91	10
6[f]	30	1.0	PhH	30	85	3
7	30	1.0	DCE	42	88	12
8[g]	30	1.0	CH_2Cl_2	45	85	12
9[h]	30	1.0	CH_2Cl_2	52	93	17
10[h]	30	0.5	CH_2Cl_2	37	—[i]	10
11[h]	30	1.5	CH_2Cl_2	56	95	18

[a] All reactions were run with 3.0 equiv. of **2a** (180 μmol) under the indicated conditions (0 °C, t = 4 h) and were initiated by addition of the oxidant PhIO (1.0 equiv.) to a pre-cooled solution of **2a** and **1** in the given solvent. [b] Concentration of quinolone **2a** in the solution. [c] All yields were determined by GLC-FID analysis using ^{n}dodecane as a stoichiometric internal standard. [d] Enantiomeric excess (% ee) as determined by HPLC analysis on a chiral stationary phase. [e] 2.0 equiv. of **2a** were employed. [f] The reaction was performed at 23 °C. [g] The reaction time was 16 h. [h] PhIO was added in three portions. [i] Not determined.

almost inconsequential for the outcome of the reaction (entry 5). Neither a solvent variation (entries 6 and 7) nor prolonged reaction times (entry 8) were found to be beneficial to conversion and enantioselectivity. A slightly higher yield of alcohol **3a** was achieved by a portion-wise addition of the oxidant (entry 9). Under these conditions a final variation of the catalyst loading (entries 10 and 11) was performed from which eventually a catalyst loading of 1.5 mol% turned out to be ideal (entry 11).

Under optimised conditions the enantiomerically enriched alcohol **3a** was isolated in 60% yield and with an enantiomeric excess of 96% ee (Table 2). Since a clean separation from both the starting material **2a** and the ketone **4a** was feasible the yield based on recovered starting material **2a** could be readily

Table 2 Scope of the enantioselective oxygenation of 3-benzylquinolone derivatives **2** catalysed by the chiral manganese porphyrin catalyst **1**

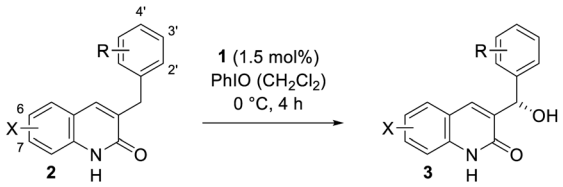

Entry[a]	**2**	X	R	**3**[b] [%]	% ee[c]
1	**2a**	H	4′-Me	60 (80)	96
2	**2b**	H	3′-Me	58 (82)	99
3	**2c**	H	2′-Me	64 (92)	97
4	**2d**	H	3′,4′-Me_2	59 (68)	92
5	**2e**	H	H	61 (84)	95
6	**2f**	H	4′-OMe	53 (74)	93
7	**2g**	H	4′-F	53 (60)	91
8	**2h**	H	4′-Cl	18 (62)	98
9	**2i**	H	3′-CF_3	26 (54)	92
10	**2j**	6-Me	4′-Me	60 (71)	98
11	**2k**	7-Me	4′-Me	53 (65)	96

[a] All reactions were conducted at a iodosobenzene concentration of 10 mM in dichloromethane employing 1.0 equiv. of PhIO (60 μmol), 3.0 equiv. of **2** (180 μmol) and 1.5 mol% of **1** (0.9 μmol). [b] All yields refer to isolated material. Yields in brackets are based on reisolated starting material **2**. [c] Enantiomeric excess (% ee) as determined by HPLC analysis on a chiral stationary phase.

determined (80%). We were interested in studying the electronic and steric effects of the benzyl substituent and accordingly prepared a series of various 3-benzylquinolones **2** which were consequentially subjected to the enantioselective oxygenation protocol. The yields in Table 2 refer to isolated material but are based on the oxidant as the limiting reagent. The yields based on substrate conversion were determined by clean reisolation of the starting material **2** and are given in brackets.

Altering the position of the methyl group to a *meta*- or *ortho*-substitution gave similar results in terms of yield (58% **3b**, 64% **3c**) and the enantiomeric excess for the corresponding alcohols **3b** and **3c** remained exceptionally high (99% ee and 97% ee). The 3′,4′-dimethylbenzyl substituted quinolone **2d** reacted almost analogously (59%), but the enantiomeric excess decreased slightly to 92% ee. The transformation of unsubstituted 3-benzylquinolone (**2e**) delivered the oxygenated product **3e** in a yield of 61% with 95% ee. An electron donating substituent (MeO) in the *para* position of the aromatic ring (**3f**, 53% yield, 93% ee) was tolerated as was an inductively electron withdrawing substituent (**3g**, 53% yield, 91% ee). Indeed, the outcome of the oxygenation seemed consistent upon variation of functional groups on the benzyl ring. A deviation was observed when 3-(4′-chlorobenzyl)quinolone (**2h**) was taken into the reaction and resulted in a low yield of only 18% (62% based on recovered starting material). While the enantioselectivity remained outstanding (98% ee), the lower conversion was attributed to the poor solubility of substrate **2h** in dichloromethane. Substrate **2i** with the strongly electron withdrawing *m*-

Open Access Article. Published on 14 January 2020. Downloaded on 2/24/2026 2:58:26 PM.
This article is licensed under a Creative Commons Attribution-NonCommercial 3.0 Unported Licence.

(trifluoromethyl)aryl substituent gave rise to the corresponding alcohol **3i** in a yield of 26% (54% based on recovered starting material) and an enantiomeric excess of 92% ee. Finally, substituents on the quinolone core were introduced into the substrates and the 6- and 7-methyl-substituted quinolones **2j** and **2k** were probed in the oxygenation event. Both substrates gave a clean conversion to the corresponding alcohols **3j** and **3k** in satisfactory yields (60% and 53%) and with remarkable enantioselectivity (98% ee and 96% ee).

In order to establish the absolute configuration of the oxygenated products, the enantiomerically enriched alcohol **3h** was subjected to a chemoselective *N*-methylation using potassium carbonate and methyl iodide in *N*,*N*-dimethylformamide (DMF) whereupon compound **5** was obtained in almost quantitative yield (Scheme 2). Colorless crystals were obtained by slow evaporation from dichloromethane which were suited for X-ray crystallographic analysis and the absolute configuration as determined by anomalous diffraction was in agreement with the proposed transition state (Fig. 2, right).

Apart from the high enantioselectivity, a most notable feature of the oxygenation reaction was its exquisite site-selectivity. When promoted by achiral Mn(TPFPP)Cl as the catalyst (2.0 mol%), substrates exhibiting a methylene group in 4′-position of the benzyl substituent [R = 4′-ethyl (**2l**); 4′-isopropyl (**2m**)] underwent a sluggish but site-selective (r.r. = regioisomeric ratio) oxygenation (Scheme 3) to the remote alcohols *rac*-**2n** (27%) and **2o** (20%). In stark contrast, catalyst **1** (1.5 mol%) guided the oxygenation reaction almost exclusively to the benzylic carbon atom adjacent to the quinolone core whereupon the oxygenated products **3l** (57%) and **3m** (50%) were obtained with excellent enantioselectivity (93% ee and 91% ee). The reversal of site-selectivity supports a pre-coordination of quinolone substrates **2** to the catalyst which in turn leads to a defined exposure of a single C–H towards the active oxomanganese[26] complex. Accordingly, non-covalent hydrogen bonding completely alters the site of the oxygenation reaction to a position that seems inaccessible by conventional oxygenation methods.

The scope of the reaction was substantially expanded by varying the size and nature of the quinolone substituent in position C-3. A brief screening of reaction conditions based on the previously developed protocol indicated that even simple 3-alkylsubstituted quinolones underwent the desired transformation (Table 3) and that an aryl group was not necessary to

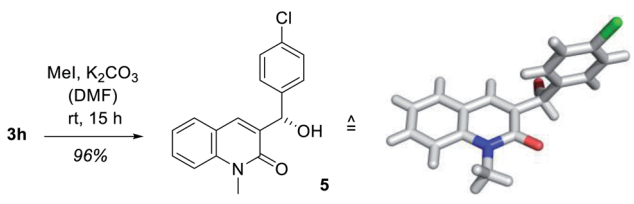

Scheme 2 Synthesis of the *N*-methylated alcohol **5** derived from 3-(4′-chlorobenzyl)-quinolone (**3h**) by chemoselective methylation and its crystal structure. The absolute configuration was determined by anomalous X-ray diffraction.

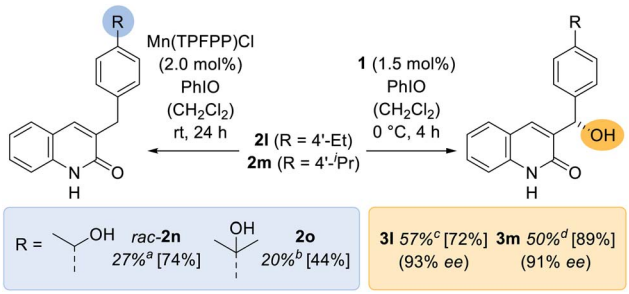

Scheme 3 Enantioselective and racemic oxygenation of quinolones **2l** and **2m** bearing an additional reactive methylene site. The racemic reaction was promoted by Mn(TPFPP)Cl (left) and the enantioselective reaction by the chiral manganese porphyrin complex **1** (right). Yields in square brackets are based on recovered starting material **2** ([a]r.r. = 93/7, [b]r.r. = 82/18, [c]r.r. = 94/6, [d]r.r. = 97/3).

activate the prostereogenic methylene group. A slightly higher catalyst loading of 2.0 mol% was required to transform 3-ethylquinolone (**6a**) into its oxygenated analogue **7a** in 56% yield and with an outstanding enantiomeric excess of 95% ee. The specific rotation of product **7a** was compared with literature data,[24a] allowing an assignment of its absolute configuration. It was interesting to see, that the formation of the corresponding ketone **8a** was less prominent (**7a**/**8a** = 88/12) than for the benzylic substrate **2a**, resulting in a high yield of 90% based on recovered starting material. Encouraged by these results, a more extensive set of 3-alkylsubstituted quinolones was prepared and

Table 3 Scope of the enantioselective oxygenation of 3-alkylquinolones **6** to alcohol **7** and ketone **8** catalysed by the chiral manganese porphyrin catalyst **1**

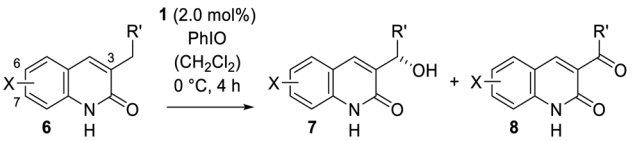

Entry[a]	6	X	R′	7[b] [%]	% ee[c]
1	**6a**	H	Me	56 (90)	95
2	**6b**	H	Et	53 (84)	88
3	**6c**	H	^{n}Pr	50 (68)	86
4	**6d**	H	^{i}Bu	48 (96)	88
5	**6e**	H	^{i}Pr	48 (89)	80
6	**6f**	6-Me	Me	51 (93)	94
7	**6g**	7-Me	Me	58 (94)	96
8	**6h**	6,7-Me$_2$	Me	51 (94)	95
9	**6i**	6-OMe	Me	21 (38)	96
10	**6j**	7-OMe	Me	62 (73)	95
11	**6k**	7-Cl	Me	34 (95)	95
12	**6l**	7-F	Me	42 (84)	96

[a] All reactions were conducted at a iodosobenzene concentration of 10 mM in dichloromethane employing 1.0 equiv. of PhIO (60 μmol), 3.0 equiv. of **6** (180 μmol) and 2.0 mol% of **1** (1.2 μmol). [b] All yields refer to isolated material. Yields in brackets are based on reisolated starting material **6**. [c] Enantiomeric excess (% ee) as determined by HPLC analysis on a chiral stationary phase.

This journal is © The Royal Society of Chemistry 2020

Open Access Article. Published on 14 January 2020. Downloaded on 2/24/2026 2:58:26 PM.
This article is licensed under a Creative Commons Attribution-NonCommercial 3.0 Unported Licence.

the effect of quinolone substitution (variation of X) was examined. Upon elongation of the alkyl chain the yield remained constant [R′ = Et (53%), ^{n}Pr (50%), ^{i}Bu (48%)], but a minor decrease in enantioselectivity was observed [**7b** (88% ee), **7c** (86% ee) **7d** (88% ee)]. This effect became even more evident when a tertiary carbon atom was installed adjacent to the oxygenation site (entry 5). The oxygenated product **7e**, derived from 3-isobutylquinolone (**6e**), was obtained in 48% yield, but only with 80% ee.

When simple methyl substituents were implemented into the aromatic quinolone core the yield of isolated product remained constant for both the C-6 and the C-7 position [X = 6-Me (51%), 7-Me (58%), 6,7-Me_2 (51%)] and the enantiomeric excess was continuously high [**7f** (94% ee), **7g** (96% ee) **7h** (95% ee)]. An electron donating methoxy substituent at the C-6 carbon atom led to a diminished yield (21%), but high enantioselectivity (96% ee) possibly due to oxidative degradation of the electron rich aryl core. The same functional group was less disruptive at the deconjugated 7-position and alcohol **7j** was obtained in 62% yield and with an enantiomeric excess of 95% ee. Electron deficient quinolones seem to be slightly less reactive [X = 7-Cl (34%), 7-F (42%)]. Nevertheless, both substrates gave rise to the desired alcohols **7k** and **7l** in again exceptional enantiomeric excess (95% ee and 96% ee).

Given the high conformational flexibility of a simple 3-ethylquinolone (**6a**), it might be surprising that hydrogen bonding can provide sufficient enantioface differentiation between the two pro-stereogenic hydrogen atoms. Rotation around the indicated single bond (Scheme 4) leads to a change of topicity even if an approach of the oxygenation reagent was guided by hydrogen bonding to occur from the back face of the quinolone. It appears as if the active manganese species behaves like a catalytically active cleft similar to the active site of a natural enzyme. It reserves only a very limited reactive domain around the oxomanganese porphyrin in which an oxygenation can occur by a rebound mechanism.[27] As previously established for the epoxidation of 3-alkenylquinolone by a chiral ruthenium complex,[24b] the trajectory of the active site to the substrate requires a perfect adjustment of the rotatable single bond. In our specific case, only the *pro*-(*S*) hydrogen atom is properly positioned to engage in oxygenation while potential transition states for the *pro*-(*R*) hydrogen atom are too high in energy to be significantly populated. Based on the proposed model (Fig. 2, right), 3-ethylquinolone in its s-*trans* conformation is aligned in a way that the oxygenation event proceeds with high selectivity at the *pro*-(*S*) hydrogen atom.

Although their outstanding stereoselectivity belongs to the most admired features of enzymatic reactions, the site-selectivity is often considered as its most useful catalytic property. As previously alluded to, molecular recognition devices cannot only help to induce enantioselectivity, but also provide a powerful tool to differentiate between two potentially reactive sites in a remote functionalization approach. This aspect was further exemplified when 3,7-diethylquinolone (**6m**) and (3′-phenylpropyl)quinolone (**6o**) were subjected to the oxygenation protocol (Scheme 5). The racemic oxygenation proceeded exclusively adjacent to the phenyl ring whereupon *rac*-**6n** (20%) and *rac*-**6p** (21%) were obtained as single regioisomers. The oxygenation site was however relocated, when the manganese porphyrin complex **1** was employed. The oxygenated product **7m** was isolated in 60% yield with almost perfect enantioselectivity (98% ee). The presented site-selective oxygenation even withstands a proximal more reactive benzylic position. (3′-Phenylpropyl)quinolone (**6o**) was converted into the corresponding alcohol **7o** with reverted site-selectivity but with a slightly reduced enantioselectivity (84% ee).

To support the hypothesis that hydrogen bonding is responsible for both the chirality transfer and for the enhanced reactivity a control experiment was performed. One hydrogen bonding site of substrate **6a** was blocked by *N*-methylation to provide quinolone **9**. When compound **9** was probed in the catalytic reaction (Scheme 6) under otherwise identical conditions its oxygenated product **10** was obtained in racemic form and a notably lower yield of 22%.

Further mechanistic work was devoted to study the over-oxidation of the enantiomerically enriched alcohol to its corresponding ketone and to elucidate the fate of the catalyst in the course of the reaction. Although a relatively high alcohol to ketone ratio clearly indicated that the enantioselectivity arises from a C–H activation step, we envisioned that detailed kinetic

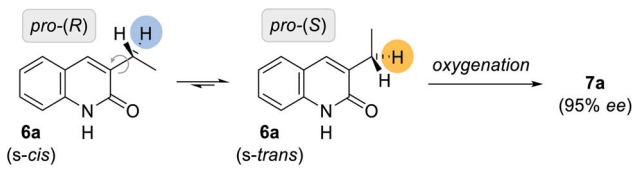

Scheme 4 Rotation around the C–C bond between the exocyclic methylene group and the quinolone carbon skeleton. Based on the proposed model, the s-*trans* isomer is favoured in the coordinated transition state whereupon the (*S*)-configured alcohol **7a** is delivered in high enantiomeric excess.

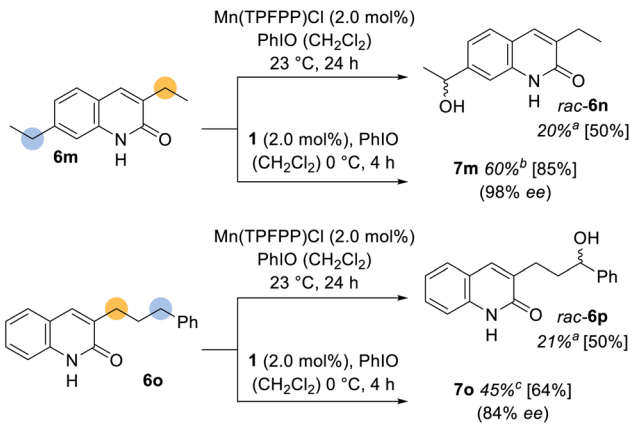

Scheme 5 Enantioselective and racemic oxygenation of 3,7-diethylquinolone (**6m**) and 3-(3′-phenylpropyl)quinolone (**6o**) using the chiral manganese porphyrin complex **1** and Mn(TPFPP)Cl, respectively. Yields in square brackets are based on recovered starting material **6** ([a]single regioisomer, [b]r.r. = 88/12, [c]r.r. = 72/28).

Open Access Article. Published on 14 January 2020. Downloaded on 2/24/2026 2:58:26 PM.
This article is licensed under a Creative Commons Attribution-NonCommercial 3.0 Unported Licence.

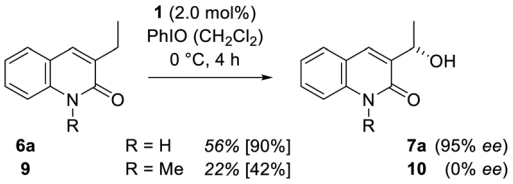

Scheme 6 Oxygenation of **6a** and the *N*-methylated congener **9** to alcohol **7a** and **10** catalysed by manganese porphyrin **1**.

studies will provide a more comprehensive mechanistic picture of the over-oxidation step. The racemic alcohol *rac*-**3a** was subjected to the oxygenation reaction (1.0 mol% **1**, 1.0 equiv. PhIO) and the formation of the ketone **4a** as well as the enantiomeric excess of the remaining starting material **3a** were closely monitored over time (Scheme 7). The rate profile derived from the experimental data indicated that after a conversion of 59% the remaining starting material **3a** was enantiomerically enriched by 71% ee (Fig. 4).

The *s*-factor[28] k_R/k_S = 6.1 calculated from these data confirmed that a kinetic resolution *via* an over-oxidation step does not contribute significantly to the enantiomeric excess.[29] Under optimised standard conditions (Table 1, entry 11) only 18% of ketone **4a** were formed but 56% of alcohol **3a** (95% ee). It is interesting to note, though, that the residual alcohol has the same absolute configuration as the alcohol derived from the C–H oxygenation step. Indeed, upon coordination of *ent*-**3a** to catalyst **1**, the remaining hydrogen atom at the former methylene group is directly exposed towards the catalytically active metal centre thus favouring an additional oxidation step *via* hydrogen abstraction.

Although all experimental data were coherent, it remained uncertain what exactly caused the rapid decrease of the catalytic activity if the quinolone substrate was used as a limiting reagent (Fig. 3). Based on detailed rate profiles, we assumed that the catalytic activity might be affected by one of the oxygenation products. To verify this hypothesis, a kinetic inhibition experiment was performed, which at the same time was supposed to shine light on the robustness of the catalyst. Quinolone **2a** was subjected towards the enantioselective oxygenation employing 1.0 mol% of the chiral catalyst **1** with 2.0 equivalents of the oxidant PhIO and the documented rate profile was used as a reference for further experiments. After 30 min 22% of the starting material **2a** had been converted into 16% of the alcohol

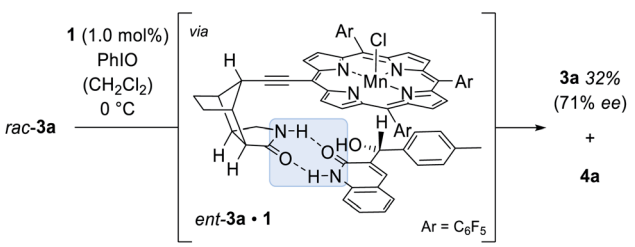

Scheme 7 Kinetic resolution of *rac*-**3a** catalysed by the chiral manganese porphyrin **1**.

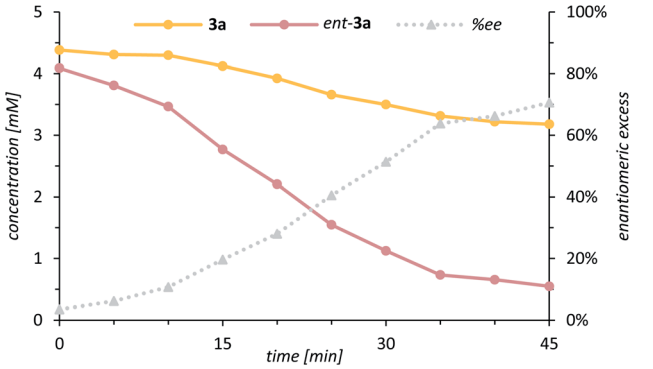

Fig. 4 Rate profile of the two enantiomers **3a** (yellow) and *ent*-**3a** (pink) in the kinetic resolution of *rac*-**3a** to ketone **4a** and enantiomeric excess (grey, dashed line) of the remaining enantiomer **3a**.

3a and 5% of the ketone **4a** (Fig. 5, solid lines). Within the next 90 min the concentration of all reactants remained almost constant (<5% conversion) clearly indicating that the catalytic activity had decreased drastically. A second oxygenation experiment was set up, in which the concentration of all reactants strictly followed the "same excess" approach.[30] Specifically, a reaction mixture containing the exact stoichiometry of all reactants **2a**, **3a** and **4a** after 60 min of the previous experiment was treated with 1.0 mol% of catalyst **1** and eventually the oxidant PhIO was added to the pre-cooled reaction mixture. The oxygenation reaction was expected to remain idle and no further conversion of the starting material **2a** should occur if the catalytic system was inhibited either by alcohol **3a** or by ketone **4a**. Upon addition of the oxidant to the premixed reaction solution, however, the oxygenation was initiated and 15% of **2a** were converted into 10% of alcohol **3a** and 7% of ketone **4a** within the next hour (Fig. 5, dashed lines).

In fact, the experiment demonstrated, that there is no inhibition by neither of the products **3a** or **4a** suggesting that after 30 min the catalyst is eventually modified resulting in a significantly diminished activity. This observation was further

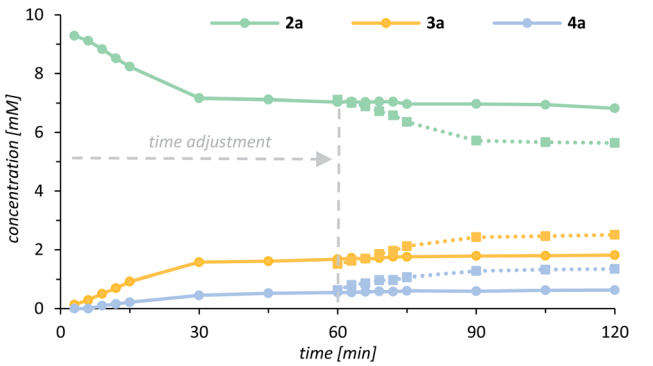

Fig. 5 Rate profile for the enantioselective oxygenation of **2a** (green) to alcohol **3a** (yellow) and ketone **4a** (blue) catalysed by the chiral manganese porphyrin complex **1** (solid lines). Overlay of the rate profile for the kinetic inhibition experiment following the "same excess" protocol[30] with a time adjustment of 60 min (dashed lines).

This journal is © The Royal Society of Chemistry 2020

Open Access Article. Published on 14 January 2020. Downloaded on 2/24/2026 2:58:26 PM.
This article is licensed under a Creative Commons Attribution-NonCommercial 3.0 Unported Licence.

corroborated by a third experiment, which was set up as usual with 1.0 equivalent of the quinolone substrate and 1.0 mol% of the catalyst **1**. The reaction was initiated by addition of the oxidant (2.0 equiv.) and – as expected – ceased after 30 min at a conversion of 24%. Upon addition of a second portion of the catalyst **1** (1.0 mol% after 60 min) the reaction was resumed and another 19% of **2a** were converted into 11% of the alcohol **3a** and 8% of the ketone **4a** conclusively matching the rate profile of the "same excess" experiment. It should be noted that the reaction was only relaunched by addition of catalyst, while addition of another portion iodosobenzene turned out to be inconsequential.

With respect to all rate profiles (see the ESI† for a complete set of data), it is conspicuous that the rapid decrease in catalytic activity correlated to the iodosobenzene concentration. At high concentration, with the quinolone as the limiting reagent, the manganese catalyst quickly lost its activity resulting in retarded conversion of the substrate to the alcohol **2a** → **3a** and of the alcohol to the ketone **3a** → **4a** (Fig. 3). In other words, the reaction slowed down but continued to show the typical rate profile of a consecutive reaction in which the alcohol is an intermediate *en route* to the ketone. The alcohol to ketone ratio **3a**/**4a** decreased over time, irrespective of catalyst and oxidant concentration. For example, after prolonged reaction times the ratio **3a**/**4a** after 1 h under the conditions of Scheme 1 (2.0 mol% **1**, 1.0 equiv. of **2a**, 2.0 equiv. PhIO) was 76/24 while it decreased to 38/62 after 24 h. In stark contrast, at a low iodosobenzene concentration with an excess of quinolone, the activity of the catalyst remained high until almost the entire iodosobenzene was consumed. The reaction is terminated due to the lack of oxidant before larger amounts of ketone can be formed. Along these lines, it is inevitable to keep the concentration of the quinolone substrate **2a** high, if elevated turnover numbers (TONs) and reasonable yields for alcohol **3a** are prioritized over the amount of **2a** applied. Reducing the concentration of the oxidant to a minimum by portion-wise addition prevents catalyst degradation and can increase the lifetime of the catalyst. Under optimized reaction conditions, high TONs and excellent yields based on recovered starting material (up to 96%) were observed, while the enantioselectivity was maintained (up to 99% ee).

Conclusion

In summary, we have established that a manganese porphyrin complex linked to a chiral recognition site effectively catalyses a highly selective oxygen insertion into a variety of aliphatic and benzylic exocyclic methylene groups. A lactam recognition motif was employed which limits the scope of substrates to compounds with a matching hydrogen bonding site. In the present study, a comprehensive set of 3-substituted quinolones (27 examples, up to 64% yield) was successfully oxygenated adjacent to the 3-position of the heterocyclic carbon skeleton with outstanding site- and enantioselectivity (up to 99% ee). Catalyst **1** operates under the influence of two-point hydrogen bonding, whereupon the substrate is precisely oriented in a way that allows for no other than the *pro*-(*S*) hydrogen atom to be attacked. Kinetic experiments revealed that employing the oxidant as the limiting reagent can significantly increase the number of catalytic turnovers and improve the alcohol to ketone ratio thus providing excellent yields based on recovered starting material.

Conflicts of interest

There are no conflicts to declare.

Acknowledgements

Financial support by the Deutsche Forschungsgemeinschaft (grant Ba 1372-17) is gratefully acknowledged. O. Ackermann and J. Kudermann are acknowledged for their help with HPLC and GLC analysis. We thank M. Stierle for synthetic assistance.

Notes and references

1 For reviews on C–H activation, see: (*a*) P. Gandeepan, T. Müller, D. Zell, G. Cera, S. Warratz and L. Ackermann, *Chem. Rev.*, 2019, **119**, 2192–2452; (*b*) C. G. Newton, S.-G. Wang, C. C. Oliveira and N. Cramer, *Chem. Rev.*, 2017, **117**, 8908–8976; (*c*) J. F. Hartwig and M. A. Larsen, *ACS Cent. Sci.*, 2016, **2**, 281–292; (*d*) H. M. L. Davies and D. Morton, *J. Org. Chem.*, 2016, **81**, 343–350; (*e*) J. Wencel-Delord, T. Dröge, F. Liu and F. Glorius, *Chem. Soc. Rev.*, 2011, **40**, 4740–4761; (*f*) L. McMurray, F. O'Hara and M. J. Gaunt, *Chem. Soc. Rev.*, 2011, **40**, 1885–1898; (*g*) K. Godula and D. Sames, *Science*, 2006, **312**, 67–72; (*h*) G. Dyker, *Handbook of C–H transformations: applications in organic synthesis*, Wiley-VCH, 2005; (*i*) J. A. Labinger and J. E. Bercaw, *Nature*, 2002, **417**, 507–514.

2 For reviews on site-selective C–H functionalization, see: (*a*) F. D. Toste, M. S. Sigman and S. J. Miller, *Acc. Chem. Res.*, 2017, **50**, 609–615; (*b*) L. Ping, D. S. Chung, J. Bouffard and S.-g. Lee, *Chem. Soc. Rev.*, 2017, **46**, 4299–4328; (*c*) S. R. Neufeldt and M. S. Sanford, *Acc. Chem. Res.*, 2012, **45**, 936–946; (*d*) T. Brückl, R. D. Baxter, Y. Ishihara and P. S. Baran, *Acc. Chem. Res.*, 2012, **45**, 826–839; (*e*) W. R. Gutekunst and P. S. Baran, *Chem. Soc. Rev.*, 2011, **40**, 1976–1991.

3 For reviews on the C–H oxygenation reactions, see: (*a*) G. B. Shul'pin, *Catalysts*, 2016, **6**, 50; (*b*) E. P. Talsi and K. P. Bryliakov, *Coord. Chem. Rev.*, 2012, **256**, 1418–1434; (*c*) T. Newhouse and P. S. Baran, *Angew. Chem., Int. Ed.*, 2011, **50**, 3362–3374; (*d*) R. Curci, L. D'Accolti and C. Fusco, *Acc. Chem. Res.*, 2006, **39**, 1–9; (*e*) L. Que and W. B. Tolman, *Nature*, 2008, **455**, 333–340; (*f*) M. Costas, M. P. Mehn, M. P. Jensen and L. Que, *Chem. Rev.*, 2004, **104**, 939–986.

4 For a recent example on a selective benzylic mono-oxygenation, see: L. Tanwar, J. Börgel and T. Ritter, *J. Am. Chem. Soc.*, 2019, **141**, 17983–17988.

5 For reviews on cytochrome P450 and bioengineered congeners, see: (*a*) T. L. Poulos, *Chem. Rev.*, 2014, **114**, 3919–3962; (*b*) R. Fasan, *ACS Catal.*, 2012, **2**, 647–666; (*c*) J. C. Lewis, P. S. Coelho and F. H. Arnold, *Chem. Soc. Rev.*,

Open Access Article. Published on 14 January 2020. Downloaded on 2/24/2026 2:58:26 PM. This article is licensed under a Creative Commons Attribution-NonCommercial 3.0 Unported Licence.

2011, **40**, 2003–2021; (*d*) P. R. Ortiz de Montellano, *Chem. Rev.*, 2010, **110**, 932–948; (*e*) P. R. Ortiz de Montellano, *Cytochrome P450: structure, mechanism, and biochemistry*, Springer Science & Business Media, 2005.

6 For reviews on metal–salen complexes, see: (*a*) K. C. Gupta and A. K. Sutar, *Coord. Chem. Rev.*, 2008, **252**, 1420–1450; (*b*) N. S. Venkataramanan, G. Kuppuraj and S. Rajagopal, *Coord. Chem. Rev.*, 2005, **249**, 1249–1268; (*c*) T. Katsuki, *Coord. Chem. Rev.*, 1995, **140**, 189–214.

7 Selected examples: (*a*) K. Hamachi, R. Irie and T. Katsuki, *Tetrahedron Lett.*, 1996, **37**, 4979–4982; (*b*) T. Hamada, R. Irie, J. Mihara, K. Hamachi and T. Katsuki, *Tetrahedron*, 1998, **54**, 10017–10028; (*c*) S.-I. Murahashi, S. Noji and N. Komiya, *Adv. Synth. Catal.*, 2004, **346**, 195–198.

8 For reviews on metalloporphyrins, see: (*a*) H. Lu and X. P. Zhang, *Chem. Soc. Rev.*, 2011, **40**, 1899–1909; (*b*) M. Costas, *Coord. Chem. Rev.*, 2011, **255**, 2912–2932; (*c*) C.-M. Che, V. K.-Y. Lo, C.-Y. Zhou and J.-S. Huang, *Chem. Soc. Rev.*, 2011, **40**, 1950–1975; (*d*) M. Senge, *Chem. Commun.*, 2011, **47**, 1943–1960.

9 Selected examples: (*a*) J. T. Groves and P. Viski, *J. Am. Chem. Soc.*, 1989, **111**, 8537–8538; (*b*) J. T. Groves and P. Viski, *J. Org. Chem.*, 1990, **55**, 3628–3634; (*c*) R. Zhang, W.-Y. Yu, T.-S. Lai and C.-M. Che, *Chem. Commun.*, 1999, 1791–1792; (*d*) Z. Gross and S. Ini, *Org. Lett.*, 1999, **1**, 2077–2080; (*e*) R. Zhang, W.-Y. Yu and C.-M. Che, *Tetrahedron: Asymmetry*, 2005, **16**, 3520–3526; (*f*) H. Srour, P. L. Maux and G. Simonneaux, *Inorg. Chem.*, 2012, **51**, 5850–5856.

10 For a recent overview of iron aminopyridine complexes, see: G. Olivo, O. Cussó and M. Costas, *Chem.–Asian J.*, 2016, **11**, 3148–3158.

11 Selected examples: (*a*) M. S. Chen and M. C. White, *Science*, 2007, **318**, 783–787; (*b*) P. E. Gormisky and M. C. White, *J. Am. Chem. Soc.*, 2013, **135**, 14052–14055; (*c*) M. Milan, M. Bietti and M. Costas, *ACS Cent. Sci.*, 2017, **3**, 196–204; (*d*) B. Qiu, D. Xu, Q. Sun, C. Miao, Y.-M. Lee, X.-X. Li, W. Nam and W. Sun, *ACS Catal.*, 2018, **8**, 2479–2487; (*e*) M. C. White and J. Zhao, *J. Am. Chem. Soc.*, 2018, **140**, 13988–14009; (*f*) R. V. Ottenbacher, E. P. Talsi, T. V. Rybalova and K. P. Bryliakov, *ChemCatChem*, 2018, **10**, 5323–5330; (*g*) J. Zhao, T. Nanjo, E. C. de Lucca and M. C. White, *Nat. Chem.*, 2019, **11**, 213–221; (*h*) B. Qiu, D. Xu, Q. Sun, J. Lin and W. Sun, *Org. Lett.*, 2019, **21**, 618–622.

12 For reviews on catalysis based on non-covalent interactions, see: (*a*) H. J. Davis and R. J. Phipps, *Chem. Sci.*, 2017, **8**, 864–877; (*b*) A. J. Neel, M. J. Hilton, M. S. Sigman and F. D. Toste, *Nature*, 2017, **543**, 637–646; (*c*) M. Raynal, P. Ballester, A. Vidal-Ferran and P. W. N. M. van Leeuwen, *Chem. Soc. Rev.*, 2014, **43**, 1660–1733; (*d*) P. Dydio and J. N. H. Reek, *Chem. Sci.*, 2014, **5**, 2135–2145; (*e*) S. Carboni, C. Gennari, L. Pignataro and U. Piarulli, *Dalton Trans.*, 2011, **40**, 4355–4373; (*f*) E. Lindbäck, S. Dawaigher and K. Wärnmark, *Chem.–Eur. J.*, 2014, **20**, 13432–13481; (*g*) S. Das, G. W. Brudvig and R. H. Crabtree, *Chem. Commun.*, 2008, 413–424.

13 (*a*) R. Breslow, *Acc. Chem. Res.*, 1980, **13**, 170–177; (*b*) R. Breslow, A. B. Brown, R. D. McCullough and P. W. White, *J. Am. Chem. Soc.*, 1989, **111**, 4517–4518; (*c*) R. Breslow, X. Zhang, R. Xu, M. Maletic and R. Merger, *J. Am. Chem. Soc.*, 1996, **118**, 11678–11679.

14 (*a*) J. T. Groves and R. Neumann, *J. Am. Chem. Soc.*, 1987, **109**, 5045–5047; (*b*) J. T. Groves and R. Neumann, *J. Org. Chem.*, 1988, **53**, 3891–3893; (*c*) J. T. Groves and R. Neumann, *J. Am. Chem. Soc.*, 1989, **111**, 2900–2909.

15 (*a*) S. Das, C. D. Incarvito, R. H. Crabtree and G. W. Brudvig, *Science*, 2006, **312**, 1941–1943; (*b*) S. Das, G. W. Brudvig and R. H. Crabtree, *J. Am. Chem. Soc.*, 2008, **130**, 1628–1637.

16 (*a*) D. Font, M. Canta, M. Milan, O. Cussó, X. Ribas, R. J. M. Klein Gebbink and M. Costas, *Angew. Chem., Int. Ed.*, 2016, **55**, 5776–5779; (*b*) G. Olivo, G. Farinelli, A. Barbieri, O. Lanzalunga, S. Di Stefano and M. Costas, *Angew. Chem., Int. Ed.*, 2017, **56**, 16347–16351; (*c*) G. Olivo, G. Capocasa, O. Lanzalunga, S. Di Stefano and M. Costas, *Chem. Commun.*, 2019, **55**, 917–920.

17 D. S. Kemp and K. S. Petrakis, *J. Org. Chem.*, 1981, **46**, 5140–5143.

18 Selected examples on hydrogen bond-mediated molecular recognition induced by a similar structural motif: (*a*) J. Rebek, K. Williams, K. Parris, P. Ballester and K. S. Jeong, *Angew. Chem., Int. Ed.*, 1987, **26**, 1244–1245; (*b*) J. Rebek, B. Askew, P. Ballester, C. Buhr, S. Jones, D. Nemeth and K. Williams, *J. Am. Chem. Soc.*, 1987, **109**, 5033–5035; (*c*) K. Williams, B. Askew, P. Ballester, C. Buhr, K. S. Jeong, S. Jones and J. Rebek, *J. Am. Chem. Soc.*, 1989, **111**, 1090–1094; (*d*) R. K. Castellano, V. Gramlich and F. Diederich, *Chem.–Eur. J.*, 2002, **8**, 118–129; (*e*) R. Faraoni, R. K. Castellano, V. Gramlich and F. Diederich, *Chem. Commun.*, 2004, 370–371; (*f*) D. B. Varshney, X. Gao, T. Friščić and L. R. MacGillivray, *Angew. Chem., Int. Ed.*, 2006, **45**, 646–650.

19 For reviews on hydrogen bond-mediated catalysis, see: (*a*) N. R. Mote and S. H. Chikkali, *Chem.–Asian J.*, 2018, **13**, 3623–3646; (*b*) X. Fang and C.-J. Wang, *Chem. Commun.*, 2015, **51**, 1185–1197; (*c*) X. Yu and W. Wang, *Chem.–Asian J.*, 2008, **3**, 516–532; (*d*) A. G. Doyle and E. N. Jacobsen, *Chem. Rev.*, 2007, **107**, 5713–5743; (*e*) M. S. Taylor and E. N. Jacobsen, *Angew. Chem., Int. Ed.*, 2006, **45**, 1520–1543; (*f*) P. R. Schreiner, *Chem. Soc. Rev.*, 2003, **32**, 289–296.

20 For recent examples, see: (*a*) Y. Park and S. Chang, *Nat. Catal.*, 2019, **2**, 219–227; (*b*) J.-P. Berndt, Y. Radchenko, J. Becker, C. Logemann, D. R. Bhandari, R. Hrdina and P. R. Schreiner, *Chem. Sci.*, 2019, **10**, 3324–3329; (*c*) X. Lu, Y. Yoshigoe, H. Ida, M. Nishi, M. Kanai and Y. Kuninobu, *ACS Catal.*, 2019, **9**, 1705–1709; (*d*) S.-T. Bai, V. Sinha, A. M. Kluwer, P. R. Linnebank, Z. Abiri, P. Dydio, M. Lutz, B. de Bruin and J. N. H. Reek, *Chem. Sci.*, 2019, **10**, 7389–7398; (*e*) S. T. Bai, C. B. Bheeter and J. N. H. Reek, *Angew. Chem., Int. Ed.*, 2019, **58**, 13039–13043; (*f*) W. Fang and B. Breit, *Angew. Chem., Int. Ed.*, 2018, **57**, 14817–14821; (*g*) X. Li, C. You, Y. Yang, Y. Yang, P. Li, G. Gu, L. W. Chung, H. Lv and X. Zhang, *Chem. Sci.*, 2018, **9**, 1919–1924; (*h*) H. J. Davis, G. R. Genov and R. J. Phipps, *Angew. Chem.,*

 This journal is © The Royal Society of Chemistry 2020

Open Access Article. Published on 14 January 2020. Downloaded on 2/24/2026 2:58:26 PM.
This article is licensed under a Creative Commons Attribution-NonCommercial 3.0 Unported Licence.

Int. Ed., 2017, **56**, 13351–13355; (*i*) Z. Han, P. Li, Z. Zhang, C. Chen, Q. Wang, X.-Q. Dong and X. Zhang, *ACS Catal.*, 2016, **6**, 6214–6218.

21 For reviews on bioinspired oxygenation, see: (*a*) D. Vidal, G. Olivo and M. Costas, *Chem.–Eur. J.*, 2018, **24**, 5042–5054; (*b*) M. Milan, M. Bietti and M. Costas, *Chem. Commun.*, 2018, **54**, 9559–9570.

22 For seminal work on hydrogen bond-mediated molecular recognition utilizing a related lactam, see: (*a*) D. G. Lonergan, J. Riego and G. Deslongchamps, *Tetrahedron Lett.*, 1996, **37**, 6109–6112; (*b*) D. G. Lonergan, J. Halse and G. Deslongchamps, *Tetrahedron Lett.*, 1998, **39**, 6865–6868; (*c*) D. G. Lonergan and G. Deslongchamps, *Tetrahedron*, 1998, **54**, 14041–14052.

23 For a recent perspective, see: F. Burg and T. Bach, *J. Org. Chem.*, 2019, **84**, 8815–8836.

24 (*a*) P. Fackler, C. Berthold, F. Voss and T. Bach, *J. Am. Chem. Soc.*, 2010, **132**, 15911–15913; (*b*) P. Fackler, S. M. Huber and T. Bach, *J. Am. Chem. Soc.*, 2012, **134**, 12869–12878; (*c*) F. Zhong and T. Bach, *Chem.–Eur. J.*, 2014, **20**, 13522–13526.

25 (*a*) T. Höke, E. Herdtweck and T. Bach, *Chem. Commun.*, 2013, **49**, 8009–8011; (*b*) J. R. Frost, S. M. Huber, S. Breitenlechner, C. Bannwarth and T. Bach, *Angew. Chem., Int. Ed.*, 2015, **54**, 691–695; (*c*) F. Burg, M. Gicquel, S. Breitenlechner, A. Pöthig and T. Bach, *Angew. Chem., Int. Ed.*, 2018, **57**, 2953–2957.

26 For mechanistic studies on the Mn-oxo species, see: (*a*) F. De Angelis, N. Jin, R. Car and J. T. Groves, *Inorg. Chem.*, 2006, **45**, 4268–4276; (*b*) W. J. Song, M. S. Seo, S. DeBeer George, T. Ohta, R. Song, M.-J. Kang, T. Tosha, T. Kitagawa, E. I. Solomon and W. Nam, *J. Am. Chem. Soc.*, 2007, **129**, 1268–1277; (*c*) N. Jin, M. Ibrahim, T. G. Spiro and J. T. Groves, *J. Am. Chem. Soc.*, 2007, **129**, 12416–12417; (*d*) S. Fukuzumi, N. Fujioka, H. Kotani, K. Ohkubo, Y.-M. Lee and W. Nam, *J. Am. Chem. Soc.*, 2009, **131**, 17127–17134; (*e*) X. Wu, M. S. Seo, K. M. Davis, Y.-M. Lee, J. Chen, K.-B. Cho, Y. N. Pushkar and W. Nam, *J. Am. Chem. Soc.*, 2011, **133**, 20088–20091; (*f*) D. F. Leto, R. Ingram, V. W. Day and T. A. Jackson, *Chem. Commun.*, 2013, **49**, 5378–5380; (*g*) M. Guo, M. S. Seo, Y.-M. Lee, S. Fukuzumi and W. Nam, *J. Am. Chem. Soc.*, 2019, **141**, 12187–12191.

27 (*a*) M. Guo, T. Corona, K. Ray and W. Nam, *ACS Cent. Sci.*, 2019, **5**, 13–28; (*b*) X. Huang and J. T. Groves, *Chem. Rev.*, 2018, **118**, 2491–2553; (*c*) X. Huang and J. T. Groves, *J. Biol. Inorg Chem.*, 2017, **22**, 185–207; (*d*) W. Liu, M.-J. Cheng, R. J. Nielsen, W. A. Goddard and J. T. Groves, *ACS Catal.*, 2017, **7**, 4182–4188; (*e*) C. Arunkumar, Y.-M. Lee, J. Y. Lee, S. Fukuzumi and W. Nam, *Chem.–Eur. J.*, 2009, **15**, 11482–11489; (*f*) B. Meunier, S. P. de Visser and S. Shaik, *Chem. Rev.*, 2004, **104**, 3947–3980; (*g*) J. T. Groves and M. Van der Puy, *J. Am. Chem. Soc.*, 1976, **98**, 5290–5297; (*h*) J. T. Groves and G. A. McClusky, *J. Am. Chem. Soc.*, 1976, **98**, 859–861.

28 (*a*) H. Kagan and J. Fiaud, *Topics in Stereochemistry*, John Wiley and Sons, Inc., New York, 1988; (*b*) J. M. Keith, J. F. Larrow and E. N. Jacobsen, *Adv. Synth. Catal.*, 2001, **343**, 5–26.

29 For non-enzymatic examples and reviews on the kinetic resolution of racemic alcohols with high *s*-factors, see: (*a*) B. Tao, J. C. Ruble, D. A. Hoic and G. C. Fu, *J. Am. Chem. Soc.*, 1999, **121**, 5091–5092; (*b*) S. Hashiguchi, A. Fujii, J. Takehara, T. Ikariya and R. Noyori, *J. Am. Chem. Soc.*, 1995, **117**, 7562–7563; (*c*) S. Hashiguchi, A. Fujii, K. J. Haack, K. Matsumura, T. Ikariya and R. Noyori, *Angew. Chem., Int. Ed.*, 1997, **36**, 288–290; (*d*) S. Y. Lee, J. M. Murphy, A. Ukai and G. C. Fu, *J. Am. Chem. Soc.*, 2012, **134**, 15149–15153; (*e*) H. Pellissier, *Adv. Synth. Catal.*, 2011, **353**, 1613–1666; (*f*) C. E. Müller and P. R. Schreiner, *Angew. Chem., Int. Ed.*, 2011, **50**, 6012–6042.

30 (*a*) D. G. Blackmond, *Angew. Chem., Int. Ed.*, 2005, **44**, 4302–4320; (*b*) J. S. Mathew, M. Klussmann, H. Iwamura, F. Valera, A. Futran, E. A. C. Emanuelsson and D. G. Blackmond, *J. Org. Chem.*, 2006, **71**, 4711–4722; (*c*) D. G. Blackmond, *J. Am. Chem. Soc.*, 2015, **137**, 10852–10866.